Nonlinear free-carrier absorption of intense THz radiation in semiconductors



2000 J. Phys.: Condens. Matter 12 4655

(http://iopscience.iop.org/0953-8984/12/21/309)

J. Phys.: Condens. Matter **12** (2000) 4655–4664. Printed in the UK PII: S0953-8984(00)11185-3

# Nonlinear free-carrier absorption of intense THz radiation in semiconductors

X L Lei†‡ and S Y Liu‡

† Department of Applied Physics, Shanghai Siaotong University, Shanghai 200050, China
‡ State Key Laboratory of Functional Materials for Informatics, Shanghai Institute of Metallurgy, Chinese Academy of Sciences, 865 Changning Road, Shanghai 200050, China

Received 20 January 2000

**Abstract.** We calculate the nonlinear free-carrier absorption coefficient of an intense terahertz (THz) electromagnetic wave propagating in a bulk semiconductor and the absorption percentage when an intense THz radiation passes through a quasi-two-dimensional (2D) sheet, with the help of the balance-equation approach to hot-electron transport in semiconductors subject to an intense high-frequency field. We find that at frequency around 1 THz, the absorption coefficient in a bulk GaAs system increases with increasing amplitude of the radiation field from zero and reaches a maximum at around 8 kV $cm^{-1}$ before decreasing quickly with further increase of the field strength. The absorption percentage of a quasi-2D system exhibits an even stronger nonlinearity than that of a three-dimensional bulk. It is shown that high-order multiphoton processes play a major role in determining the absorption of an intense THz field.

## 1. Introduction

Absorption of electromagnetic radiation by semiconductors through intraband transition of carriers, i.e. the so-called free-carrier absorption, as one of the two distinctive absorption processes in semiconductors, has been extensively studied experimentally and theoretically in the past [1, 2]. So far, however, almost all classical and quantum mechanical treatments on this problem were based on the perturbation expansion of the interaction between electrons and photons, mostly with only the single-photon process included, and thus limited to the case of weak radiation fields.

The development of the free-electron laser technique provides a tunable source of linearly polarized far-infrared or terahertz (THz) electromagnetic radiation of high intensity, and has prompted extensive experimental studies on the nonlinear dynamics of semiconductors irradiated by intense THz electromagnetic fields. People are frequently dealing with the propagation of intense THz electromagnetic waves in semiconductors. There is thus an urgent need for a clear understanding of how the propagation and absorption of a high-intensity THz electromagnetic wave differs from those for low intensity.

When an intense electromagnetic wave of THz frequency propagates in a semiconductor, the perturbative treatment of electron–photon interaction will no longer be valid and the carrier intraband transitions may occur through multiphoton process. The absorption rate may differ significantly from that in the case of a weak electromagnetic wave, and vary with changing intensity of the THz field.

0953-8984/00/214655+10$30.00  

Recently, nonperturbative approaches have been proposed to deal with interaction between intense THz radiations and carriers in three- and two-dimensional semiconductors [3, 4]. These approaches provide convenient tools for investigating the nonlinear behaviour of the absorption due to the large amplitude of the field and resulting from multiphoton emission and absorption channels. In this paper we report a systematic study on the free-carrier absorption of intense electromagnetic radiations of terahertz frequency in three-dimensional (3D) and quasi-two-dimensional (2D) semiconductors, with the help of the balance-equation approach [4] to hot-electron transport in semiconductors subject to an intense terahertz field.

## 2. Balance-equation treatment of interaction between THz radiation and semiconductors

We consider a carrier system consisting of $n_{\rm e}$ electrons with effective mass $m$ and charge $e$, moving in an isotropic semiconductor of unit volume, and assume that a dc electric field $\boldsymbol{E}_0$ and a uniform sinusoidal radiation field of frequency $\omega$ and amplitude $\boldsymbol{E}_\omega$, $\boldsymbol{E}_\omega \sin(\omega t)$, are applied in the system. These electric fields, which are in arbitrary directions and of arbitrary strengths, can be described by a vector potential $\boldsymbol{A}(t)$ and a scalar potential $\varphi(\boldsymbol{r})$ of the form

$$\boldsymbol{A}(t) = (\boldsymbol{E}_\omega/\omega)\cos(\omega t) \tag{1}$$

$$\varphi(\boldsymbol{r}) = -\boldsymbol{r}\cdot\boldsymbol{E}_0. \tag{2}$$

With these potentials, we can separate the centre-of-mass motion from the relative motion of electrons [5] and distinguish the slowly varying part from the rapidly oscillating part of the centre-of-mass velocity when the frequency of the radiation field is in, or above, the THz range. Considering the fact that relevant transport quantities are measured over a time interval much longer than the period of the THz field, we obtain a set of momentum and energy balance equations, without invoking a perturbational treatment of the electron–photon interaction [4]. These equations, which include the elastic (zero-) photon process and all orders of multiphoton emission and absorption processes, state the momentum and energy balances on a timescale much longer than the period of the THz field after the system has reached the steady transport state:

$$n_{\rm e}e\boldsymbol{E}_0 + \boldsymbol{f} = 0 \tag{3}$$

$$s_{\rm p} - \boldsymbol{v}_0\cdot\boldsymbol{f} - w = 0. \tag{4}$$

Here, $\boldsymbol{v}_0$ is the average drift velocity of electrons, $\boldsymbol{f}$ is the average frictional force experienced by the centre of mass due to impurity and phonon scatterings in the presence of the THz radiation field, $w$ is the average rate of energy transfer from the electron system to the phonon system, and $s_{\rm p}$ is the average rate of energy gain of the electron system from the radiation field associated with carrier intraband transition through impurity- and phonon-assisted, single- and multiphoton (absorption and emission) processes. The last quantity is given by [4]

$$\begin{aligned} s_{\rm p} = n_{\rm i}\sum_{\boldsymbol{q}}|u(\boldsymbol{q})|^2\sum_{n=-\infty}^{\infty}J_n^2(\boldsymbol{q}\cdot\boldsymbol{r}_\omega)n\omega\Pi_2(\boldsymbol{q},\boldsymbol{q}\cdot\boldsymbol{v}_0-n\omega) \\ + 2\sum_{\boldsymbol{q},\lambda}|M(\boldsymbol{q},\lambda)|^2\sum_{n=-\infty}^{\infty}J_n^2(\boldsymbol{q}\cdot\boldsymbol{r}_\omega)n\omega \\ \times\,\Pi_2(\boldsymbol{q},\Omega_{\boldsymbol{q}\lambda}+\boldsymbol{q}\cdot\boldsymbol{v}_0-n\omega)\left[n\left(\frac{\Omega_{\boldsymbol{q}\lambda}}{T}\right)-n\left(\frac{\Omega_{\boldsymbol{q}\lambda}+\boldsymbol{q}\cdot\boldsymbol{v}_0-n\omega}{T_{\rm e}}\right)\right]. \end{aligned} \tag{5}$$

The expression for $\boldsymbol{f}$ is obtained from the right-hand side of equation (5) by replacing the $n\omega$ factor with wavevector $\boldsymbol{q}$ in both terms, and the expression for $w$ is obtained from the second term on the right-hand side of equation (5) by replacing the $n\omega$ factor with $\Omega_{q\lambda}$. Here, $\boldsymbol{r}_\omega \equiv e\boldsymbol{E}_\omega/(m\omega^2)$, $J_n(x)$ is the Bessel function of order $n$, $n_{\rm i}$ is the impurity density, $u(\boldsymbol{q})$ is the electron–impurity potential and $M(\boldsymbol{q}, \lambda)$ is the electron–phonon matrix element, $\Omega_{q\lambda}$ is the energy of a phonon having wavevector $\boldsymbol{q}$ in branch $\lambda$,

$$n(x) \equiv 1/[\exp(x) - 1]$$

is the Bose function, and $\Pi_2(\boldsymbol{q}, \Omega)$ is the imaginary part of the electron density–density correlation function in an equilibrium state at the electron temperature $T_{\rm e}$, which is generally different from the lattice temperature $T$.

It should be noted that in writing $s_{\rm p}$, $\boldsymbol{f}$, and $w$ in a form like equation (5), we have somewhat mixed the contributions from absorption and emission processes of photons to get a compact expression. Thus, in equation (5), the part with negative (positive) values of the summation index $n$ does not imply a pure emission (absorption) process. The combination of both $n$- and $-n$-terms, of course, represents the total (net) contribution to $s_{\rm p}$ from the $n$-photon ($n \geqslant 1$) emission and absorption processes. We therefore write $s_{\rm p}$ as a sum of all orders of $n$-photon contributions:

$$s_{\rm p} = \sum_{n=1}^{\infty} s_{\rm p}^{(n)} \tag{6}$$

where $s_{\rm p}^{(n)}$ is the total contribution from terms having indices $n$ and $-n$ in equation (5).

## 3. Nonlinear absorption coefficient of a THz radiation in a bulk semiconductor

The quantity $s_{\rm p}$ defined in equation (5) represents the average energy of the radiation field which is absorbed in unit time by the carriers in the system of unit volume. We consider, in the semiconductor, a small cylindrical element having its axis parallel to the propagating direction of the radiation field and volume $\Delta\tau = \Delta S\,\Delta z$ ($\Delta S$ and $\Delta z$ are respectively the area of the upper/lower surface and the height of the cylinder). The average rate of electromagnetic radiation energy flow into the small volume is $\frac{1}{2}v\kappa\epsilon_0 E_\omega^2\,\Delta S$, in which $v = c/\sqrt{\kappa}$ is the propagating velocity of the electromagnetic wave in the semiconductor, $c$ is the speed of light in vacuum, and $\kappa$ is the dielectric constant of the material. The energy of the radiation field, which is absorbed in unit time by the carriers inside the small volume, $s_{\rm p}\,\Delta S\,\Delta z$, is just the energy loss of the electromagnetic wave after propagating a distance $\Delta z$. Therefore, the absorption coefficient is given by

$$\alpha = \frac{2}{\sqrt{\kappa}\epsilon_0 c}\frac{s_{\rm p}}{E_\omega^2}. \tag{7}$$

In the limit of weak high-frequency field (small $E_\omega$), the argument $\boldsymbol{q}\cdot\boldsymbol{r}_\omega$ of the Bessel functions on the right-hand side of the $s_{\rm p}$-expression (5) is small. It suffices, for the calculation of $s_{\rm p}$, to retain the single-photon process ($n = 1$ and $-1$) and keep just the leading terms of the expansion of the Bessel function: $J_{\pm1}^2 \approx \frac{1}{4}(\boldsymbol{q}\cdot\boldsymbol{r}_\omega)^2$. We have

$$\alpha = \frac{1}{\sqrt{\kappa}\epsilon_0 c}\frac{n_{\rm e}e^2}{m\omega^2}M_2(\omega, \boldsymbol{v}_0) \tag{8}$$

where $M_2(\omega, \boldsymbol{v}_0)$ is the imaginary part of the memory function $M(\omega, \boldsymbol{v}_0)$ under a dc bias velocity $\boldsymbol{v}_0$, which consists of contributions from impurity and phonon scatterings:

$$M_2(\omega, \boldsymbol{v}_0) = M_2^{(\rm i)}(\omega, \boldsymbol{v}_0) + M_2^{(\rm p)}(\omega, \boldsymbol{v}_0) \tag{9}$$

with the impurity part $M_2^{(\mathrm{i})}(\omega, \boldsymbol{v}_0)$ and phonon part $M_2^{(\mathrm{p})}(\omega, \boldsymbol{v}_0)$ given respectively by

$$M_2^{(\mathrm{i})}(\omega, \boldsymbol{v}_0) = \frac{n_\mathrm{i}}{n_\mathrm{e} m\omega} \sum_{\boldsymbol{q}} |u(\boldsymbol{q})|^2 q_\omega^2 \Pi_2(\boldsymbol{q}, \boldsymbol{q}\cdot\boldsymbol{v}_0 - \omega) \tag{10}$$

$$M_2^{(\mathrm{p})}(\omega, \boldsymbol{v}_0) = \frac{1}{n_\mathrm{e} m\omega} \sum_{\boldsymbol{q},\lambda} |M(\boldsymbol{q}, \lambda)|^2 q_\omega^2 \big\{ \Pi_2(\boldsymbol{q}, \Omega_{\boldsymbol{q}\lambda} + \boldsymbol{q}\cdot\boldsymbol{v}_0 - \omega) \times \big[n(\Omega_{\boldsymbol{q}\lambda}/T) - n((\Omega_{\boldsymbol{q}\lambda} + \boldsymbol{q}\cdot\boldsymbol{v}_0 - \omega)/T_\mathrm{e})\big] - (\omega \to -\omega)\big\} \tag{11}$$

where $q_\omega$ stands for the component of $\boldsymbol{q}$ along the $\boldsymbol{E}_\omega$-direction. $M_2^{(\mathrm{i})}(\omega, \boldsymbol{v}_0)$ and $M_2^{(\mathrm{p})}(\omega, \boldsymbol{v}_0)$ depend on the scattering matrix element, the frequency of the radiation field, the magnitude of $\boldsymbol{v}_0$, and the relative direction of $\boldsymbol{v}_0$ and $\boldsymbol{E}_\omega$.

Expression (8) for the absorption coefficient of a weak radiation field is in agreement with the previous perturbation theory result for the free-carrier absorption, which is equivalent to the high-frequency ($\omega\tau \gg 1$) result for the extended Drude-type formula for the dynamic conductivity under a dc bias [6–8]:

$$\sigma(\omega) = \frac{n_\mathrm{e} e^2}{m} \frac{\mathrm{i}}{\omega + M(\omega, \boldsymbol{v}_0)} = \frac{\mathrm{i} n_\mathrm{e} e^2}{m^*(\omega + \mathrm{i}/\tau)} \tag{12}$$

where $m^* = m[1 + M_1(\omega, \boldsymbol{v}_0)/\omega]$ and $1/\tau = M_2(\omega, \boldsymbol{v}_0)/[1 + M_1(\omega, \boldsymbol{v}_0)/\omega]$, with $M_1(\omega, \boldsymbol{v}_0)$ being the real part of the memory function $M(\omega, \boldsymbol{v}_0)$.

In the case of an intense high-frequency field, the absorption coefficient given by equation (7) depends on the amplitude of the high-frequency field. To calculate this nonlinear absorption coefficient, one needs to solve the steady-state momentum and energy balance equations (3) and (4) before obtaining $\boldsymbol{v}_0$, $T_\mathrm{e}$, and the pertinent energy absorption rate $s_\mathrm{p}$ for using in the general expression (7). In the absence of a dc bias field, however, it suffices to solve the energy balance equation

$$w - s_\mathrm{p} = 0 \tag{13}$$

to obtain the electron temperature $T_\mathrm{e}$ and the pertinent $s_\mathrm{p}$, for using in calculating the absorption coefficient $\alpha$.

As an example, we have performed numerical calculations at lattice temperature $T = 150$ K for a model n-type GaAs system having electrons of density $n_\mathrm{e} = 10^{23}$ m$^{-3}$ moving in a parabolic $\Gamma$ valley. Elastic scattering is assumed due to randomly distributed charged impurities with density $n_\mathrm{i}$ equal to the electron density (this results in a 4.2 K linear mobility $\mu_0 = 8$ m$^2$ V$^{-1}$ s$^{-1}$). The nonelastic scatterings are due to polar optic phonons (via Fröhlich coupling with electrons), longitudinal acoustic phonons (via deformation potential and piezoelectric coupling), and transverse acoustic phonons (via piezoelectric coupling with electrons). The material and electron–phonon coupling parameters are taken as typical values for GaAs. For the absence of a dc bias, the calculated electron temperature $T_\mathrm{e}$ and nonlinear absorption coefficient $\alpha$ are plotted respectively in figure 1(a) and figure 1(b) as functions of the wavelength $\lambda$ (or frequency $\omega/2\pi$) of the radiation field, for vanishingly small $E_\omega$ (linear case) and several finite strengths $E_\omega = 0, 5, 7, 10, 12$, and 14 kV cm$^{-1}$. The electron temperature $T_\mathrm{e}$ monotonically increases with increasing $E_\omega$ and/or increasing $\lambda$. The absorption coefficient $\alpha$ for these intense fields, on the other hand, can be higher or lower than the linear absorption coefficient (as shown in figure 1(b) by the chain line). Its wavelength dependence deviates markedly from that in the linear case. At fixed frequency, the absorption coefficient increases with increasing amplitude of the radiation field from $E_\omega = 0$, then reaches a maximum at around 7–14 kV cm$^{-1}$ before decreasing quickly with further increase of $E_\omega$, as shown in the inset of figure 1(b).

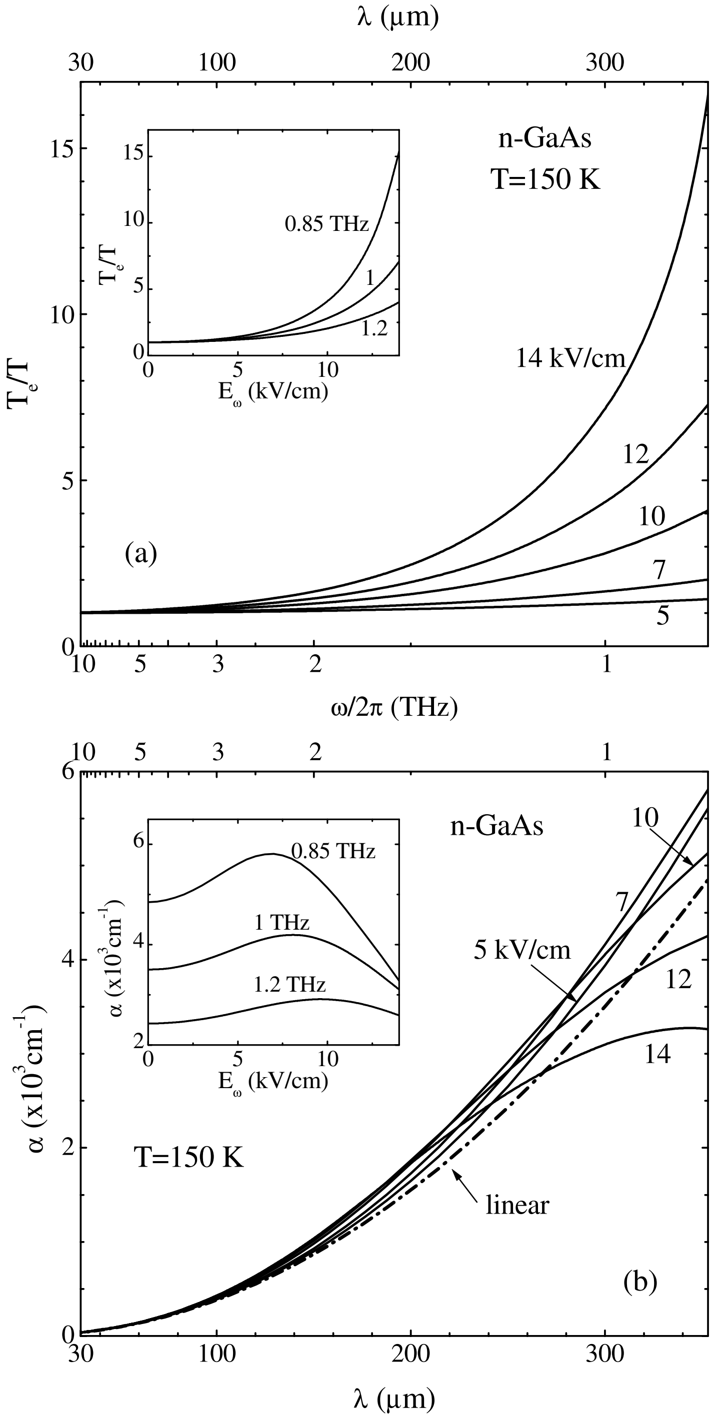


**Figure 1.** The electron temperature $T_e$ and the absorption coefficient $\alpha$ of bulk GaAs subject to a THz radiation in the absence of a dc bias are plotted as functions of the wavelength $\lambda$ (or frequency $\omega/2\pi$) of the radiation field for vanishing (chain line) and several finite amplitudes $E_\omega = 5, 7, 10, 12$, and 14 kV cm$^{-1}$ (solid lines). The lattice temperature is $T = 150$ K. The insets show $T_e$ versus $E_\omega$ (in figure 1(a)) and $\alpha$ versus $E_\omega$ (in figure 1(b)) at several fixed frequencies.

To see the role of individual multiphoton processes, we define

$$\alpha_n \equiv \frac{2}{\sqrt{\kappa}\epsilon_0 c}\frac{s_{\rm p}^{(n)}}{E_\omega^2} \tag{14}$$

to be the contribution of the $n$-photon (absorption and emission) process to the absorption coefficient: $\alpha = \sum_{n=1}^{\infty} \alpha_n$. For a set amplitude, $E_\omega = 10$ kV cm$^{-1}$, the $n$-photon contributions $\alpha_n$ ($n = 1, 2, 3, 5$, and 10) are plotted in figure 2 as functions of the wavelength λ (or frequency $\omega/2\pi$) of the radiation field, together with the total absorption coefficient $\alpha$ ($\alpha_4, \alpha_6, \ldots$ are not shown in the figure for clarity). For a set frequency, $\omega/2\pi = 1.2$ THz, the $n$-photon contributions $\alpha_n$ ($n = 1, 2, 3, 5$, and 10) and the total absorption coefficient $\alpha$ are shown in figure 3 as functions of the amplitude $E_\omega$ of the radiation field.

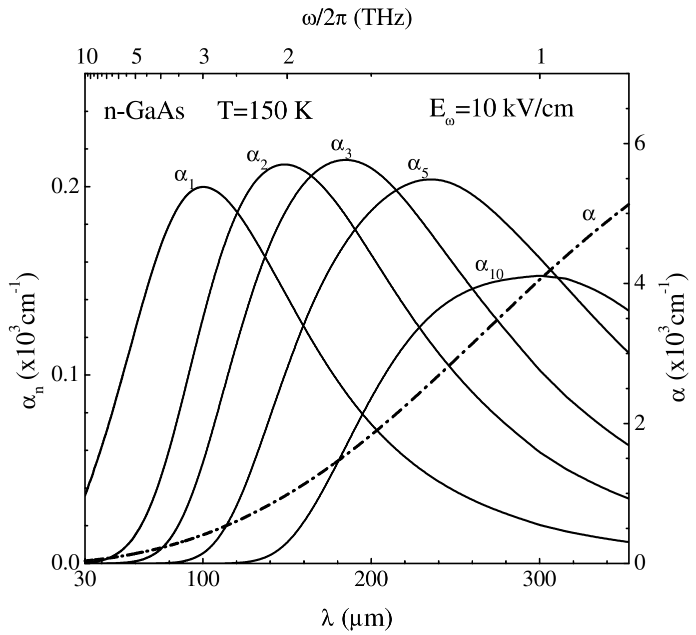


**Figure 2.** The $n$-photon contributions $\alpha_n$ ($n = 1, 2, 3, 5$, and 10) and the total absorption coefficient $\alpha$ versus the wavelength of the radiation field λ at a fixed amplitude $E_\omega = 10$ kV cm$^{-1}$, for the 3D system shown in figure 1.

It is seen from figure 2 that, although the single-photon process dominates for $E_\omega \leqslant 1$ kV cm$^{-1}$, its contribution decreases quickly with increasing $E_\omega$, and multiphoton ($n \geqslant 2$) processes play a more important role when $E_\omega \geqslant 2$ kV cm$^{-1}$. At intense radiation fields, i.e. $E_\omega \sim 10$ kV cm$^{-1}$, high orders of multiphoton processes play a decisive role; even the $n$-photon channels with $n$ as large as 300 cannot be neglected if one is to get an accurate result.

## 4. Rate of absorption of a THz radiation passing through a 2D sheet

For a quasi-2D system with the single-electron state described by a 2D (in the $x$–$y$ plane) wavevector $\boldsymbol{k}_\parallel = (k_x, k_y)$ and a subband index $s$, the energy dispersion reads

$$\varepsilon_s(\boldsymbol{k}_\parallel) = \varepsilon_s + k_\parallel^2/2m. \tag{15}$$

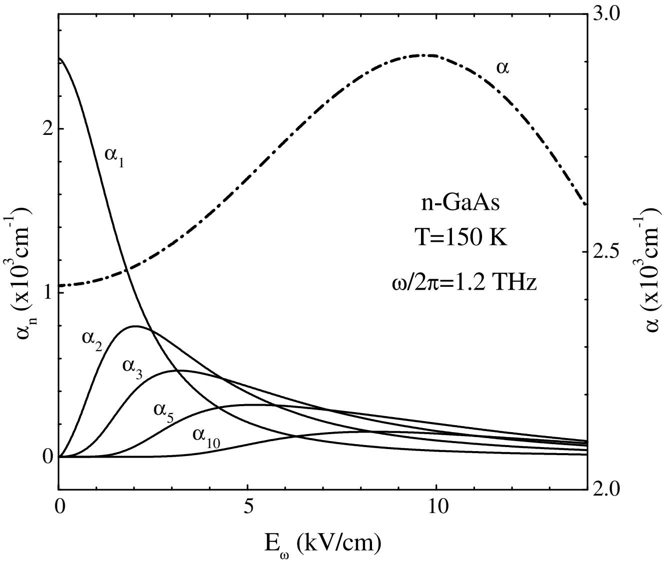


**Figure 3.** The $n$-photon contributions $\alpha_n$ ($n = 1, 2, 3, 5$, and 10) and the total absorption coefficient $\alpha$ versus the amplitude $E_\omega$ of radiation field at a set frequency, $\omega/2\pi = 1.2$ THz, for the 3D system shown in figure 1.

Here, $\varepsilon_s$ denotes the bottom of the $s$th subband. Under the influence of a dc and a high-frequency radiation field (parallel to the 2D plane), the steady-state balance equations for a 2D system having unit area can be written as [4]

$$N_s e \boldsymbol{E}_0 + \boldsymbol{F} = 0 \tag{16}$$

$$S_p - \boldsymbol{v}_0 \cdot \boldsymbol{F} - W = 0. \tag{17}$$

Here, $N_s$ is the sheet density of electrons, $\boldsymbol{v}_0$ is the average drift velocity, $\boldsymbol{F}$ is the average frictional force, $W$ is the average rate of energy transfer to the phonon system, and $S_p$ is the average rate of energy gain from the radiation field, for the quasi-2D system having unit area. The expression for $S_p$ is [4]

$$\begin{aligned} S_p = \sum_{s,s',\boldsymbol{q}_\parallel} |U_{s,s'}(\boldsymbol{q}_\parallel)|^2 \sum_{n=-\infty}^{\infty} J_n^2(\boldsymbol{q}_\parallel \cdot \boldsymbol{r}_\omega) n\omega \Pi_2(s, s', \boldsymbol{q}_\parallel, \boldsymbol{q}_\parallel \cdot \boldsymbol{v}_0 - n\omega) \\ + 2 \sum_{s,s',\boldsymbol{q},\lambda} |M_{s,s'}(\boldsymbol{q}, \lambda)|^2 \sum_{n=-\infty}^{\infty} J_n^2(\boldsymbol{q}_\parallel \cdot \boldsymbol{r}_\omega) n\omega \\ \times \Pi_2(s, s', \boldsymbol{q}_\parallel, \Omega_{\boldsymbol{q}\lambda} + \boldsymbol{q}_\parallel \cdot \boldsymbol{v}_0 - n\omega) \left[ n\left(\frac{\Omega_{\boldsymbol{q}\lambda}}{T}\right) - n\left(\frac{\Omega_{\boldsymbol{q}\lambda} + \boldsymbol{q}_\parallel \cdot \boldsymbol{v}_0 - n\omega}{T_e}\right)\right]. \end{aligned} \tag{18}$$

The expression for $\boldsymbol{F}$ is obtained from the right-hand side of equation (18) by replacing the $n\omega$ factor with $\boldsymbol{q}_\parallel$ in both terms, and the expression for $W$ is obtained from the second term of the right-hand side of equation (18) by replacing the $n\omega$ factor with $\Omega_{\boldsymbol{q}\lambda}$ (assuming the phonon modes are the same as for 3D GaAs). Here, $\boldsymbol{q} = (\boldsymbol{q}_\parallel, q_z)$ is the 3D wavevector, $U_{s,s'}(\boldsymbol{q}_\parallel)$ is an effective impurity potential, $M_{s,s'}(\boldsymbol{q}, \lambda)$ is the electron–phonon matrix element, and $\Pi_2(s, s', \boldsymbol{q}_\parallel, \Omega)$ is the imaginary part of the electron-density correlation function, related to subbands $s$ and $s'$. Their explicit expressions were given in reference [9].

For quasi-2D systems, we can use the ratio of the energy loss of the electromagnetic radiation after passing through the 2D sheet to the energy of the electromagnetic wave impinging into the system as a measure of the absorption of the radiation. We call it the absorption percentage and also denote it by $\alpha$. In the case of perpendicular incidence ($\boldsymbol{E}_\omega$ parallel to the 2D plane), the absorption percentage is given by

$$\alpha = \frac{2}{\sqrt{\kappa}\epsilon_0 c}\frac{S_{\rm p}}{E_\omega^2}. \tag{19}$$

The small-$E_\omega$ limit of the 2D absorption percentage can also be expressed in terms of 2D memory functions [10] similar to those for the 3D results (equations (8) to (12)). For the case of a finite amplitude of the radiation field, we have carried out numerical calculations for a GaAs-based quantum well having well width $a = 12.5$ nm and electron density $N_{\rm s} = 5.5 \times 10^{15}$ m$^{-2}$. We consider polar optical phonon and longitudinal and transverse acoustic phonon scatterings as in the 3D case. The elastic scattering is assumed to be due to charged impurities located at a distance of 40 nm from the centre plane of the well, with an impurity density such that the low-temperature (4.2 K) linear mobility of the system equals $\mu_0 = 31$ m$^2$ V$^{-1}$ s$^{-1}$. We consider the role of the lowest two subbands ($s = 0, 1$). The energy separation between the zeroth and the first subband bottoms, $\varepsilon_{10} \equiv \varepsilon_1 - \varepsilon_0$, is taken to be 69 meV.

The calculated absorption percentage $\alpha$ at lattice temperature $T = 150$ K, in the absence of a dc bias, is shown in figure 4 as a function of wavelength $\lambda$ or frequency $\omega/2\pi$ of the radiation field for several different field strengths, $E_\omega = 5, 7, 10, 12$, and 14 kV cm$^{-1}$, as well

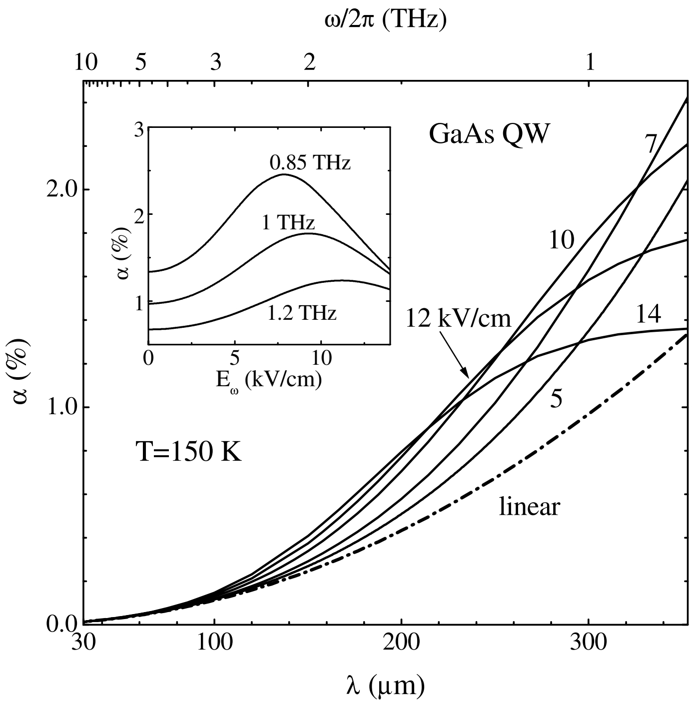


**Figure 4.** The absorption percentage $\alpha$ of a THz radiation passing through the 2D sheet of a GaAs-based quantum well described in the text, in the absence of dc bias, is plotted as a function of the wavelength $\lambda$ (or frequency $\omega/2\pi$) of the radiation field for vanishing (chain line) and several finite amplitudes $E_\omega = 5, 7, 10, 12$, and 14 kV cm$^{-1}$ (solid lines). The lattice temperature is $T = 150$ K. The inset shows $\alpha$ versus $E_\omega$ at several fixed frequencies.

as for vanishing $E_\omega$ (chain line). The absorption percentage of the GaAs quantum well exhibits a stronger nonlinearity than that for bulk GaAs. The maxima showing up in the $\alpha$-versus-$E_\omega$ curves, for fixed frequencies, are higher than in the 3D case (see the inset of figure 4).

The $n$-photon contributions to the absorption percentage, $\alpha_n$ ($n = 1, 2, 3, 5$, and 10), are plotted in figure 5 as functions of $\lambda$ (or $\omega/2\pi$) for fixed $E_\omega = 10$ kV cm$^{-1}$, and in figure 6 as functions of $E_\omega$ for fixed frequency $\omega/2\pi = 1.2$ THz, together with the total absorption percentage $\alpha$. The role of the $n$th multiphoton process in quasi-2D systems is similar to that in 3D systems. The single-photon process dominates only when $E_\omega \leqslant 1$ kV cm$^{-1}$. At higher strength of the radiation field, multiphoton ($n \geqslant 2$) channels provide major contributions to the absorption.

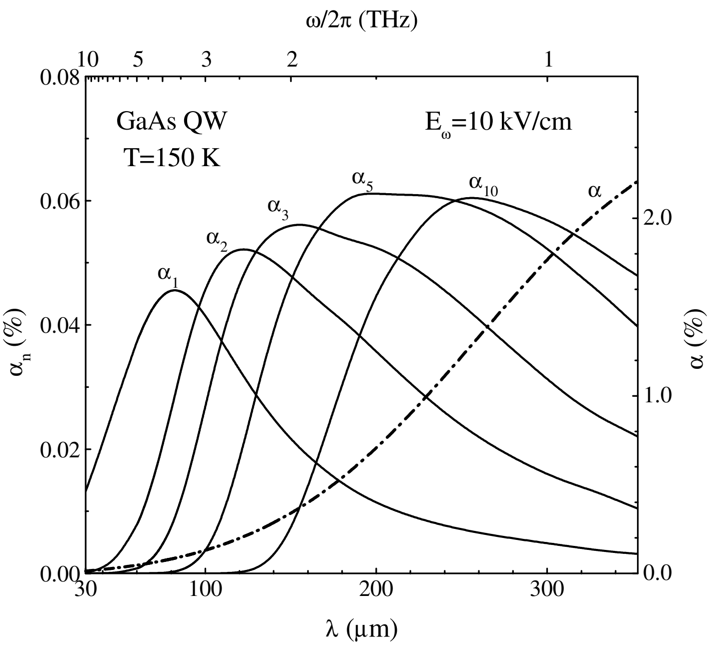


**Figure 5.** The $n$-photon contributions $\alpha_n$ ($n = 1, 2, 3, 5$, and 10) and the total absorption percentage $\alpha$ are plotted against the wavelength $\lambda$ of the radiation field at a fixed amplitude $E_\omega = 10$ kV cm$^{-1}$, for the quantum well system described in the text.

## 5. Conclusions

The free-carrier absorption coefficient of a THz electromagnetic wave propagating in a bulk semiconductor and the absorption percentage when a THz radiation passes through a quasi-two-dimensional (2D) sheet have been calculated, using the balance-equation approach to hot-electron transport in semiconductors subject to an intense high-frequency field. The absorption of THz radiation in semiconductors exhibits significantly nonlinear behaviour when the strength of the radiation field gets as high as, or higher than, a few kV cm$^{-1}$. The absorption nonlinearity is stronger at lower frequency than at higher frequency. At frequency around 1 THz, the absorption coefficient of a bulk GaAs system increases with increasing amplitude of the radiation field from zero and reaches a maximum at around 8 kV cm$^{-1}$ before decreasing quickly with further increase of the field strength. The absorption percentage of a

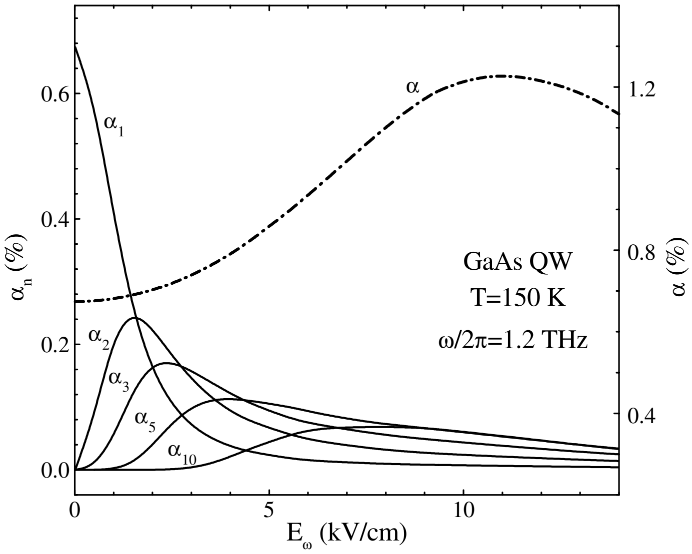


**Figure 6.** The $n$-photon contributions $\alpha_n$ ($n = 1, 2, 3, 5$, and 10) and the total absorption percentage $\alpha$ are plotted against the amplitude $E_\omega$ of the radiation field at a set frequency, $\omega/2\pi = 1.2$ THz, for the quantum well system described in the text.

quasi-2D system exhibits an even stronger nonlinearity than that of a 3D bulk. The high-order multiphoton channels provide major contributions to the nonlinear absorption of an intense THz field.

## Acknowledgments

This work was supported by the National Natural Science Foundation of China, the Ministry of Science and Technology of China, the Shanghai Municipal Commission of Science and Technology, and the Shanghai Foundation for Research and Development of Applied Materials.

## References


[1] Nag B R 1980 *Electron Transport in Compound Semiconductors* (Berlin: Springer)
[2] Butcher P N and Cotter D 1990 *Elements of Nonlinear Optics* (Cambridge: Cambridge University Press)
[3] Xu W 1998 *Phys. Rev.* B **57** 12 939
Xu W 1998 *Phys. Rev.* B **57** 15 282
Xu W 1998 *Europhys. Lett.* **44** 62
[4] Lei X L 1998 *J. Appl. Phys.* **84** 1396
Lei X L 1998 *J. Phys.: Condens. Matter* **10** 3201
[5] Lei X L and Ting C S 1985 *Phys. Rev.* B **32** 1112
[6] Götze W and Wöfle P 1972 *Phys. Rev.* B **6** 122
[7] Ting C S, Ying S C and Quinn J J 1976 *Phys. Rev. Lett.* **37** 215
[8] Zou Z Q and Lei X L 1995 *Phys. Rev.* B **50** 9493
[9] Lei X L 1985 *J. Appl. Phys.* **58** 2270
[10] Lei X L, Horing N J M and Zhang J Q 1986 *Phys. Rev.* B **33** 2912